

Relaxation of photoinduced spins and carriers in ferromagnetic InMnSb films

K. Nontapot, R. N. Kini, A. Gifford, T. R. Merritt, and G. A. Khodaparast^{a)}
Department of Physics, Virginia Tech, Blacksburg, Virginia 24061

T. Wojtowicz
Institute of Physics, Polish Academy of Sciences, 02-668 Warsaw, Poland

X. Liu and J. K. Furdyna
Department of Physics, University of Notre Dame, Notre Dame, Indiana 46556

(Received 7 November 2006; accepted 27 February 2007; published online 4 April 2007)

The authors report time resolved measurements and control of photoinduced spin and carrier relaxations in InMnSb ferromagnetic films with 2% Mn content (grown by low-temperature molecular beam epitaxy) using femtosecond laser pulses, and compare them to analogous measurements on InBeSb and InSb films. In this work, magneto-optical Kerr effect and standard pump-probe techniques provided a direct measure of the photoexcited spin and carrier lifetimes, respectively. They observe decrease in relaxations times in the high laser fluence regime and an absence of temperature dependence of the relaxation times. © 2007 American Institute of Physics. [DOI: 10.1063/1.2719173]

Current research activities in the area of ferromagnetic semiconductor have been mainly focused on III-Mn-V alloys with small lattice constants and large effective masses of valence band such as GaMnAs,¹⁻⁴ where the highest values of the Curie temperature (T_C) have been achieved so far. Various theoretical models have been proposed to explain the actual mechanism of ferromagnetism in III-Mn-V but the microscopic mechanism is still a matter of controversy.^{1,5-10} In particular, much has been said regarding the inverse correlation of T_C and the lattice parameter, which has led to considerable research on GaMnN and related alloys. It is therefore important in this context to explore the opposite extreme of the III-Mn-V ternaries, i.e., InMnSb,^{11,12} which has the largest lattice constant in this family of materials. In spite of its low T_C , InMnSb has significant potential for application in infrared spin photonics and in spin transport devices because it has the smallest effective mass of the holes, and thus a much higher hole mobility than the other III-Mn-V ferromagnetic semiconductors. It is also unique in having the smallest energy gap among the ferromagnetic III-Mn-V. Recent Andreev reflection measurements suggest up to 52% spin polarization in ferromagnetic InMnSb, thus this material maybe of special interest as a source of spin-polarized carriers.¹³

Most current understanding of the InMnSb system is gleaned from static magnetization and electrical transport measurements.¹¹⁻¹⁵ Here we report spin/carrier relaxation measurements on III-Mn-V narrow gap system grown by molecular beam epitaxy technique.¹⁶ We measure the above relaxations using femtosecond laser pulses with two different energies per pulse, resulting in different laser fluences and therefore different photoinduced carrier densities. We compare our results with recent time resolved measurements on other narrow gap semiconductor ferromagnetic systems, such as InMnAs with 9% (Ref. 17) and InGaMnAs (Refs. 17 and

18) with 5% Mn contents where only high laser fluence regimes were tested. The measured spin/carrier relaxation times in our InMnSb samples do not demonstrate strong temperature dependence. A similar lack of temperature dependence in spin relaxation has been reported in (Ga,Mn)As with a 2% Mn concentration.⁴ The sensitivity of magnetic order to the hole density due to strong $p-d$ exchange coupling between holes and the embedded localized magnetic moments has been demonstrated experimentally.¹⁹⁻²³ Another aspect of the observation in this work is that the relaxation lifetime depends on (and can thus be controlled by) the density of the photoinduced carriers. The Elliot-Yafet mechanism²⁴ is considered to be the dominant relaxation process in narrow gap semiconductors, and in this model the spin relaxation is proportional to the momentum relaxation time, which itself depends on temperature, concentration, and mobility.

In this work, in addition to InMnSb, we have studied two nonferromagnetic low temperature (LT) grown materials, LT-InSb, and LT-InBeSb with ~1% Be concentration^{11,12} (with similar growth conditions), the comparison with which allows us to infer the effect of Mn on spin/carrier dynamics in InMnSb. The samples and their characteristics are listed in Table I, the detail of growth conditions can be found in Refs.

TABLE I. List of the samples studied. T_{Mn} is the Mn effusion's cell temperature. All samples have 0.23 μm of active layer and except LT-InSb, all are p type. The relaxation times listed are at 77 K for low laser fluence. (The relaxation time is referred to the time that the signal at positive time delay reaches approximately to the same value as the negative time delay.)

Sample	Density (cm^{-3})	Mobility ($\text{cm}^2/\text{V s}$)	Carrier lifetime (ps)	Spin lifetime (ps)	T_{Mn} ($^{\circ}\text{C}$)
InMnSb(C)	2×10^{20}	100	30	25	710
InMnSb(B)	2×10^{20}	100	15	10	700
LT-InBeSb	1.4×10^{20}	170	50	50	
LT-InSb	2×10^{18}	1000	50	50	

^{a)} Author to whom correspondence should be addressed; electronic mail: khoda@vt.edu

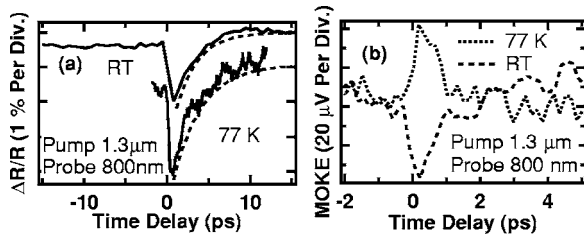


FIG. 1. Two-color measurements with pump fluence of $\sim 5 \text{ mJ/cm}^2$ of InMnSb (sample B). (a) Differential reflectivity (the dashed lines are exponential fits to the relaxations after the timing zero; for clarity the fits are displaced from the experimental traces). The differential reflectivity demonstrates an initial decrease lasting about 5 ps followed by an increase in reflectivity which shows a slow decay to its original value in the negative time delay. (b) MOKE at 77 K and room temperature. For clarity MOKE traces are plotted for two different circular polarizations of the pump.

11 and 12. The InMnSb samples studied in this work have 2% Mn concentration and $T_C \sim 9 \text{ K}$.

We measured dynamics of photoexcited carriers and their spins using standard pump/probe and magneto-optical Kerr effect (MOKE) techniques (both degenerate and two color). In the degenerate measurements, the pump was near infrared (NIR) pulses from a Ti:sapphire laser which produces tunable radiation from 750 to 850 nm with a pulse duration of $\sim 100 \text{ fs}$ at a repetition rate of 80 MHz. The maximum average power of the pump was about 400 mW (energy per pulse of $\sim 5 \text{ nJ}$). A small portion ($\sim 10\%$) of the NIR beam was split off to be used as the probe beam. In the two-color pump/probe and MOKE, the source of the pump beam was midinfrared pulses from an optical parametric amplifier pumped by a chirped pulse amplifier (CPA) with maximum average power of $\sim 1.1 \text{ W}$, a pulse energy of $\sim 1 \text{ mJ}$, and duration of $\sim 100 \text{ fs}$ at a repetition rate of 1 kHz. Small fraction ($\sim 10^{-5}$) of the CPA signal was used as a NIR source for the probe beam.

Since GaAs substrate absorbs the NIR radiation we used the reflection geometry instead of transmission to probe the dynamics as a function of time delay between the pump and the probe. The probe and pump beams were focused and overlapped on the samples in a spot size of $\sim 100\text{--}150 \mu\text{m}$ (slightly larger for the pump) inside a cryostat. We monitored Kerr signals by recording the intensity difference between the *s* and *p* components of the reflected NIR beam using a Si balanced detector and a lock-in amplifier. The pump beam was circularly polarized using a quarter wave plate to excite spin-polarized carriers. Selection rules for interband transitions suggest that spin-polarized carriers can be created using circularly polarized beams. The MOKE signal arises from the difference between the optical coefficients of a material for left and right circularly polarized lights which are proportional to the magnetization produced by the circularly polarized pump.²⁵

Here we report the results of MOKE induced by optical magnetization to measure spin relaxations. Two-color temporal traces of photoexcited MOKE and carrier relaxations signals for InMnSb (sample B) are shown in Fig. 1. The pump wavelength was fixed at $1.3 \mu\text{m}$ with an average power of 1.1 mW (pump fluence of $\sim 5 \text{ mJ/cm}^2$), resulting in the photoinduced carrier density of the order of $\sim 10^{19} \text{ cm}^{-3}$, less than the background density. The probe beam was 800 nm, with an average power of $\sim 5 \mu\text{W}$. In Fig. 1(a) the differential reflectivity signals are plotted at room temperature and

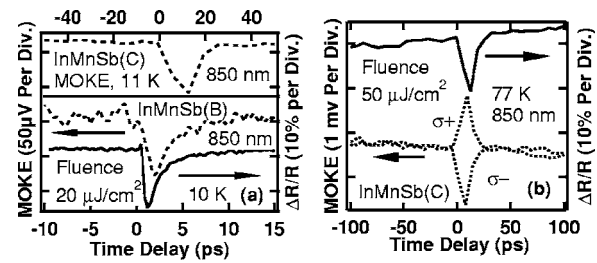


FIG. 2. (a) Differential reflectivity and MOKE of InMnSb (sample B) in the degenerate configuration at 10 K. In addition, for comparison, the MOKE signal of sample C is plotted at 11 K. (b) MOKE signal of InMnSb (sample C) for two different circularly polarized pump beams and differential reflectivity at 77 K.

77 K. Figure 1(b) shows the MOKE at 77 K and room temperature. In this regime, the MOKE signal only lasts for less than 2 ps, similar to the relaxation observed in InMnAs and InGaMnAs with a similar photoinduced carrier density.¹⁷

Figure 2(a) (the two lowest traces) demonstrates the carrier/spin dynamics of the InMnSb (sample B) using the degenerate configuration at 10 K with pump fluence of $\sim 20 \mu\text{J/cm}^2$; in addition, for comparison, the MOKE signal of sample C (the top trace) is shown at 11 K. Figure 2(b) shows the MOKE signal and the differential reflectivity of InMnSb (sample C) with pump fluence of $\sim 50 \mu\text{J/cm}^2$ using two different circular polarizations for the pump. In this pumping regime the observed spin relaxations were more than a factor of 3 longer compared to those observed with the two-color pumping regime, where the photoinduced carrier density is expected to be in the $10^{17}\text{--}10^{18} \text{ cm}^{-3}$ range.

In order to probe the effect of magnetic ordering and temperature on the relaxation time, we measured MOKE and carrier dynamics at several temperatures *below and above* the sample Curie temperature $T_C = 9 \text{ K}$. Examples of these measurements are shown in Fig. 3(a), the experimental conditions being the same as for Fig. 2(b). We were able to trace the dynamics up to room temperature. Since raising the temperature above the T_C only resulted a small modification of the relaxations, this suggests that at low Mn concentrations ($\sim 2\%$ in this case) the spin relaxation of photoexcited carriers might not be influenced by interactions with Mn ions.

As shown in Fig. 3(b), we performed carrier relaxation measurements at 77 K on LT-InBeSb and LT-InSb samples under similar experimental conditions, as in Fig. 2. The carrier relaxation of LT-InSb demonstrates a sharp increase and a slow recovery, which is clearer in this case compared to the other two alloy samples. It is known that the low-temperature growth produces large densities of point defects that act as carrier trapping centers and strongly alter the carrier lifetimes, and we observe some signatures of this effect. In InMnAs a slow recovery of $\sim 200 \text{ ps}$ in differential reflectivity has been observed where electron-hole recombination through trapping at midgap defects is considered to be responsible for the slow recovery.¹⁷ Figure 3(c) shows the results of MOKE measurements obtained on LT-InSb and LT-InBeSb, where a two-step relaxation is clearer compared to the InMnSb samples. In order to demonstrate this feature more quantitatively, we fitted exponential functions to the signals after the timing zero in Figs. 1(a), 3(b), and 3(c) to model the relaxations. In Fig. 3(c), unlike the first two cases where only a single exponential was used, we had to add two exponential functions to model the relaxations. We also ex-

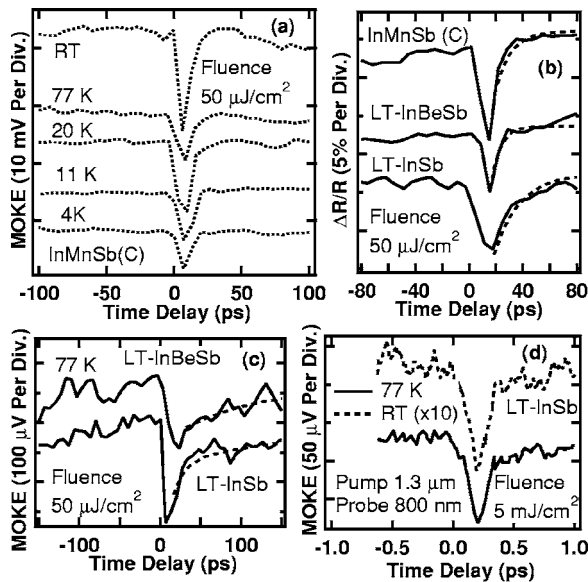


FIG. 3. (a) Photoinduced MOKE in InMnSb (sample C) at different temperatures. There is no significant difference between the relaxation above and below T_C . (b) Differential reflectivities of InMnSb, LT-InBeSb, and LT-InSb at 77 K (the dashed lines are exponential fits to the relaxations after the timing zero). (c) MOKE measurements on LT-InBeSb and LT-InSb using the degenerate pump/probe scheme at 77 K (the dashed lines are the sum of two exponential functions to the relaxations after the timing zero). (d) MOKE measurements on LT-InSb using the two-color scheme at room temperature and at 77 K.

amined the dynamic of LT-InSb in the presence of a large density of photoinduced carriers using the two-color scheme, where we observe a faster relaxation than that seen in Fig. 3(c). In addition, in this regime the LT-InSb shows a faster spin relaxation than that observed for InMnSb in Fig. 1(b).

In summary, photoinduced spin/carrier relaxation was measured and altered in LT-InSb based ferromagnetic and nonferromagnetic films in different pumping regimes. We observe faster relaxations in the case of higher laser fluences (in the two-color measurements) that produce higher photoinduced carrier densities. This fact can be explained by the Elliot-Yafet²⁴ mechanism, which is the dominant relaxation mechanism in narrow gap semiconductors. In high laser fluence regime, our observations are consistent with the measured relaxations in InMnAs and InGaMnAs (Ref. 17) where the interaction between photoinduced carriers and Mn ions is considered to be responsible for the fast relaxation (~ 1 ps). In our samples, the tunability of the relaxation times as a function of photoinduced carrier density suggests that other mechanisms such as momentum relaxation can be more crucial compared to the carrier-Mn ion interaction. In addition, in our InMnSb samples, varying the sample temperature from above to below the T_C modified the relaxations only slightly (without any anomalies at T_C), suggesting the absence of interaction of photoinduced carriers with Mn ions. Based on this and the observed long relaxation time in the low laser fluence regime (much shorter relaxations are expected for holes because of the strong spin-orbit interaction), we therefore attribute the observed photoinduced carrier/spin dynamics entirely to the relaxation of photoexcited electrons in the conduction band. In III-Mn-V ferromagnetic semiconductors, the s - d coupling with the localized Mn ions is sig-

nificantly weaker compared to the p - d exchange coupling characterizing the valence band. This effect can have important consequences for applications of InMnSb in developing spin based devices, since this alloy has much higher hole mobility than the other III-Mn-V ferromagnetic semiconductors. We are presently pursuing similar measurements in the presence of an external magnetic field to help us better understand the interaction and the differences in these materials.

This work has been supported by NSF-DMR-0507866, AFOSR Young Investigator Program 06NE231, Jeffress Trust Fund J748, Advance-VT, and NSF-DMR06-03752.

- ¹T. Dietl, H. Ohno, F. Matsukura, J. Cibert, and D. Ferrand, *Science* **287**, 1019 (2000).
- ²M. Nazmul, S. Kobayashi, S. Sugahara, and M. Tanaka, *Physica E (Amsterdam)* **21**, 937 (2004).
- ³E. Kojima, R. Shimano, Y. Hashimoto, S. Katsumoto, Y. Iye, and M. Kuwata-Gonokami, *Phys. Rev. B* **68**, 193203 (2003).
- ⁴A. V. Kimel, G. V. Astakhov, G. M. Schott, A. Kirilyuk, D. R. Yakovlev, G. Karczewski, W. Ossau, G. Schmidt, L. W. Molenkamp, and Th. Rasing, *Phys. Rev. Lett.* **92**, 237203 (2004).
- ⁵H. Akai, *Phys. Rev. Lett.* **81**, 3002 (1998).
- ⁶J. Inoue, S. Nonoyama, and H. Itoh, *Phys. Rev. Lett.* **85**, 4610 (2000).
- ⁷J. König, Hsiu-Hau Lin, and A. H. MacDonald, *Phys. Rev. Lett.* **84**, 5628 (2000).
- ⁸V. I. Litvinov and V. K. Dugaev, *Phys. Rev. Lett.* **86**, 5593 (2001).
- ⁹A. Chattopadhyay, S. Das Sarma, and A. J. Millis, *Phys. Rev. Lett.* **87**, 227202 (2001); Chattopadhyay J. Schliemann and A. H. MacDonald, *ibid.* **88**, 137201 (2002).
- ¹⁰Gergely Zaránd and Boldizsár Jankó, *Phys. Rev. Lett.* **89**, 047201 (2002).
- ¹¹T. Wojtowicz, G. Cywinski, W. L. Lim, X. Liu, M. Dobrowolska, J. K. Furdyna, K. M. Yu, W. Walukiewicz, G. B. Kim, M. Cheon, X. Chen, S. M. Wang, and H. Luo, *Appl. Phys. Lett.* **82**, 4310 (2003).
- ¹²T. Wojtowicz, W. L. Lim, X. Lim, G. Cywinski, M. Kutrowski, L. V. Titova, K. Yee, M. Dobrowolska, J. K. Furdyna, K. M. Yu, W. Walukiewicz, G. B. Kim, M. Cheon, X. Chen, S. M. Wang, H. Luo, I. Vurgaftman, and J. R. Meyer, *Physica E (Amsterdam)* **20**, 325 (2004).
- ¹³R. P. Panguluri, K. C. Ku, T. Wojtowicz, X. Liu, J. K. Furdyna, Y. B. Lyanda-Geller, N. Samarth, and B. Nadgorny, *Phys. Rev. B* **72**, 054510 (2005).
- ¹⁴M. Csontos, T. Wojtowicz, X. Liu, M. Dobrowolska, B. Jankó, J. K. Furdyna, and G. Mihály, *Phys. Rev. Lett.* **95**, 227203 (2005).
- ¹⁵M. Csontos, G. Mihály, B. Jankó, T. Wojtowicz, X. Liu, and J. K. Furdyna, *Nat. Mater.* **4**, 447 (2005).
- ¹⁶G. A. Khodaparast, K. Nontapot, A. Gifford, S. J. Chung, N. Goel, M. B. Santos, T. Wojtowicz, X. Liu, and J. K. Furdyna, *Inst. Phys. Conf. Ser.* **187**, 517 (2006).
- ¹⁷J. Wang, C. Sun, Y. Hashimoto, J. Kono, G. A. Khodaparast, Ł. Cywiński, L. J. Sham, G. D. Sanders, C. J. Stanton, and H. Munekata, *J. Phys.: Condens. Matter* **18**, R501 (2006).
- ¹⁸G. A. Khodaparast, D. C. Larrabee, J. Kono, D. S. King, J. Kato, T. Slupinski, A. Oiwa, H. Munekata, G. D. Sanders, and C. J. Stanton, *J. Appl. Phys.* **93**, 8286 (2003).
- ¹⁹H. Ohno, D. Chiba, F. Matsukura, T. Omiya, E. Abe, T. Dietl, Y. Ohno, and K. Ohtani, *Nature (London)* **408**, 944 (2000).
- ²⁰S. Koshihara, A. Oiwa, M. Hirasawa, S. Katsumoto, Y. Iye, C. Urano, H. Takagi, and H. Munekata, *Phys. Rev. Lett.* **78**, 4617 (1997).
- ²¹A. Oiwa, T. Slupinski, and H. Munekata, *Appl. Phys. Lett.* **78**, 518 (2001).
- ²²A. Oiwa, Y. Mitsumori, R. Moriya, T. Slupinski, and H. Munekata, *Phys. Rev. Lett.* **88**, 137202 (2002).
- ²³K. C. Ku, S. J. Potashnik, R. F. Wang, S. H. Chun, P. Schiffer, N. Samarth, M. J. Seong, A. Mascarenhas, E. Johnston-Halperin, R. C. Myers, A. C. Gossard, and D. D. Awschalom, *Appl. Phys. Lett.* **82**, 2302 (2003).
- ²⁴R. J. Elliot, *Phys. Rev.* **96**, 266 (1954).
- ²⁵A. K. Zvezdin and V. A. Kotov, *Modern Magneto-optics and Magneto-optical Materials* (IOP, Bristol, 1997).